ELSEVIER

Biophysical Chemistry 108 (2004) 101–119

Biophysical Chemistry

www.elsevier.com/locate/bpc

HIV Rev self-assembly is linked to a molten-globule to compact structural transition☆

Rajendran Surendran[a], Petr Herman[a], Zhijie Cheng[a], Thomas J. Daly[b], J. Ching Lee[a,*]

[a]*Department of Human Biological Chemistry and Genetics, University of Texas Medical Branch, Galveston, Texas 77555-1055, USA*

[b]*Regeneron Pharmaceutical, Inc., Tarrytown, NY 10591-6707, USA*

Abstract

By regulating the differential expression of proviral pre mRNA in the host cell, Rev plays a crucial role in the HIV-1 life cycle. The capacity of Rev to function is intimately linked to its ability to self-associate. Nevertheless, little is known about the exact role of self-association in the molecular mechanism defining its biological activity. A prerequisite knowledge is a definition of the molecular events undertaken by Rev during the process of self-assembly. Thus, this study was initiated to monitor the structure of Rev as a function of protein concentration. Rev undergoes a structural transition as a consequence of self-assembly. This structural transition was monitored by three spectroscopic methods. The accessibility of the single tryptophan in Rev monomer to acrylamide quenching increases with decreasing protein concentration. At very low concentration of Rev, the tryptophan accessibility is close to that of an unfolded Rev. As evaluated by circular dichroism, the secondary structure of Rev is protein concentration dependent as evidenced by an increase in the magnitude of ellipticity with increasing protein concentration. Further, results from ANS binding studies indicate that the ANS binding sites in Rev experience an apparent increase in hydrophobicity as the Rev concentration was increased. These concentration dependent changes seem to reach a maximum above 5 μM Rev monomer concentration. In order to define the mode of Rev self-association sedimentation velocity and equilibrium experiments were conducted. There are evidently two consecutive progressive association processes. At protein concentrations below 0.5 mg/ml, the data from sedimentation studies can be fitted to a single isodesmic model. Simulation of velocity sedimentation profile indicates that free Rev monomer that has not entered into the association processes can best be described to exhibit a value of $S_{20,w}$ that is substantially smaller than 1.4 S, a value needed to fit the rest of the data. The latter value is consistent for a Rev monomer with the expected molecules weight and if it were to assume a compact globular shape. These spectroscopic and hydrodynamic results imply that monomeric Rev is in a molten globule state, which becomes more compact upon self-association.

Keywords: HIV-1; Rev; Self-association

☆ To Professor David Yphantis whose work on sedimentation established an approach for all scientists in investigating protein hydrodynamics and assembly.

*Corresponding author. Tel.: +1-409-772-2281; fax: +1-409-772-4298.

E-mail address: jclee@utmb.edu (J. Ching Lee).

0301-4622/04/$ - see front matter © 2003 Elsevier B.V. All rights reserved.
doi:10.1016/j.bpc.2003.10.013

1. Introduction

Rev is one of the two transactivating nuclear proteins of HIV-1 responsible for differential regulation of viral mRNA in the host cell. In the absence of functional Rev, the formation of complete infectious virion is inhibited. Being a regulatory protein, Rev acts as a traffic signal in the nucleus directing the viral mRNA away from splicing to form unspliced and singly spliced viral mRNAs, which code for the structural proteins Gag and Env of matured virus [1–3]. Thus Rev, acting post-transcriptionally, controls the translocation and translation of viral mRNA. Consequently, Rev functions to ensure a completion of viral life cycle.

Rev is a basic protein of 116 amino acid residues with a molecular mass of 13 000. It is predominantly located in the nucleolus. Being involved in multiple biological functions, such as multimerization, RNA binding and interaction with host cellular proteins; Rev has a well-tailored amino acid sequence to conduct these functions [4]. Based on mutational studies, two distinct regions in Rev have been identified as required for in vivo biological activity [4]. They are the RNA and cellular factors binding regions.

Rev polymerizes to higher order structures [5–8] and the biological role of this polymerization capability is still unclear. It was reported that Rev oligomerization in solution is prerequisite for RNA binding [9–11]. Rev polymerization is not only involved in viral mRNA binding and protecting it from splicing [12–14], but also is apparently required for translocating viral mRNA to cytoplasm [15,16] for translation into viral proteins. It is conceivable that polymerized Rev interacts with host cellular factors [17–19]. Thus, reversible polymerization of Rev is of crucial importance for its biological role. An understanding of the mode of association and the structural changes in Rev that are coupled with the self-assembly process is fundamental to the elucidation of the mechanism of Rev function.

2. Experimental procedure

2.1. Materials

Escherichia coli strain RGN 714 containing the plasmid pREV 2.1 is a kind gift of Repligen Corporation. Casein hydrolysate, peptone and yeast extract were from Difco. Potassium phosphate, potassium chloride, glycerol, Tris, sodium chloride, urea, acetonitrile, DTT, EDTA, PMSF, chloramphenicol and Triton X-100 were from Sigma. Bio-Rex 70 and hydroxylapatite were obtained from Bio-Rad and CM-Sepahrose, S-Sepahrose, Sephadex LH-20 and Superdex-200 were from Pharmacia Biotech. ANS was from Kodak Laboratories and was further purified on Sephadex LH-20 before use [20].

2.2. Methods

All experiments were conducted in 10 mM potassium phosphate buffer containing 1 M sodium chloride at pH 7.4 and 20 °C unless otherwise mentioned. The absorption coefficients were 8490 M^{-1} cm^{-1} at 280 nm for Rev [1] and 6240 M^{-1} cm^{-1} for ANS [21] and were used for the spectrophotometric determination of concentrations of these regents.

2.2.1. Purification of Rev protein

Rev protein was expressed by Rev gene cloned into plasmid pREV 2.1, which was transformed into *Escherichia coli* strain RGN 714 (Repligen Corp.; 1). The *E. coli* cells were grown in broth described by Daly et al. [22] at 40 °C for 24 h in a 10 l fermentor with constant aeration. The harvested cells were stored frozen at −70 °C. *E. coli* cells were lysed by French press in 50 mM Tris–HCl buffer of pH 7.6 containing 5 mM EDTA, 1 mM PMSF, 1 mM DTT and 0.05% Triton X-100 (lysis buffer) and the clear supernatant was ethanol precipitated. This precipitate was resuspended in buffer containing 8 M urea and the clear solution was loaded onto a CM-Sepharose column equilibrated in low salt buffer with 8 M urea and eluted with a 0–0.6 M sodium chloride gradient. The eluted Rev peak fractions were applied onto a C_{18} reverse phase HPLC column, and Rev was eluted with a 0–40% acetonitrile gradient containing 0.075% trifluoroacetic acid. Fractions containing Rev were lyophilized and then solubilized in 0.01 M Tris–HCl buffer of pH 7.6 containing 8 M urea and loaded onto a S-

Sepharose column equilibrated with the same buffer. The column was washed with 0.01 M Tris–HCl buffer at pH 7.6 with no urea. The refolded protein was eluted with a 0–0.2 M sodium chloride gradient. These pure fractions were stored at 4 °C or −20 °C.

2.2.2. Velocity sedimentation

Rev was equilibrated by dialysis with 10 mM potassium phosphate buffer containing either 1 or 0.42 M sodium chloride at pH 7.4. Experiments were conducted at 20 °C at different rotor speeds, depending on the association state of Rev, in a Beckman analytical ultracentrifuge. Scans were made at regular intervals of time at various wavelengths. Weight average sedimentation coefficients were determined from the centroid. The observed weight average sedimentation coefficients were normalized to standard conditions by correcting for solvent density and viscosity. For an associating protein system of n species in a rapid, dynamic equilibrium, the rate of sedimentation of the protein boundary is defined by the velocity of the square root of the second moment of the boundary and corresponds to the weight average sedimentation coefficient, $\bar{s}$ which can be expressed as a function of total protein concentration, C, by

$$\bar{s} = \sum_i s_i^o (1 - g_i C) K_i C_1^i / \sum_i K_i C_1^i \tag{1}$$

where s_i^o is the sedimentation coefficient of the ith species at infinite dilution, g_i, is the non-ideality coefficient, $C = \sum K_i C_1^i$, K_i is the equilibrium constant between any i-mer and the monomer, and C_1 is the monomer concentration. Theoretical values of $\bar{s}$ as a function of C_1, s_i^o, g_i, and K_i can be fitted to the observed weight average sedimentation coefficients as a function of C; thus, the best fitted curve can yield information on the physical parameters which govern the multimerization reaction.

2.2.3. Simulation of velocity sedimentation profiles

Based on the method of Holloway and Cox [23] sedimentation velocity profiles in the form of derivative curves were simulated using the parameters derived from fitting of the experimental results. In this distorted grid method the ultracentrifuge cell is divided into an array of n boxes, each ΔX deep and to the midpoint of box i the weight concentration C_i is assigned. The simulation proceeds by treating the concentration array alternately with the expressions that simulate diffusion without sedimentation for a short time and then sedimentation without diffusion for an equal time. Since in this procedure the entire system is in chemical equilibrium, the total solute concentration is given by,

$$C_T = \sum_i C_i = C_1 \left[1 + 2\frac{KC_1}{M_1} + 3\left(\frac{KC_1}{M_1}\right)^2 + \cdots + i\left(\frac{KC_1}{M_1}\right)^{i-1} + \cdots \right] \tag{2}$$

Based on this, the monomer concentration (C_1) and the concentration of intermediates are defined, since

$$C_T = \frac{C_1}{(1 - KC_1)^2} \tag{3}$$

$$C_i = i\left(\frac{K_2}{2}\right)^{i-1} C_1^i \tag{4}$$

The appropriate concentration dependence of transport coefficients, namely, sedimentation and diffusion coefficients, were calculated by the relationships,

$$s_i = \frac{iM_1(1 - \bar{v}\rho)}{Nf_i} \tag{5}$$

$$D_i = \frac{RT}{Nf_i} \tag{6}$$

$$f_i = 6\pi\eta R_i^s \left(f/f_o\right)_i \tag{7}$$

$$R_i^s = \left(\frac{3iM_1\bar{v}}{4\pi N}\right)^{1/3} \tag{8}$$

$$s_i = s_1(i)^{2/3} \tag{9}$$

$$D_i = D_1(i)^{-1/3} \tag{10}$$

where M_1 is the molecular weight of the monomer, f/f_o is the frictional ratio of each species, $\bar{v}$ is partial specific volume, T is the temperature in Kelvin units, ρ is density of solvent, η is viscosity of solvent, R is gas constant, N is Avogadro's number, f_i is the frictional coefficient and R_i^s is the Stokes radius of individual species. Eqs. (9) and (10) imply that all the polymers exhibit spherical geometry. If this assumption is invalid, then these equations do not apply. Using these equations, the weight average sedimentation and diffusion coefficients in each box were calculated by employing the equation [24,25],

$$\bar{s} = \frac{\sum_i s_i C_i}{\sum_i C_i} \tag{11}$$

$$\bar{D} = \frac{\sum_i i D_i C_i}{\sum_i i C_i} \tag{12}$$

A table of $\bar{s}$ and $\bar{D}$ was made in the concentration range of zero to the initial plateau concentration using the above equations. For the total concentration in each box the $\bar{s}$ and $\bar{D}$ values were extracted by interpolation from the table. The simulations started by calculating C_i in each box and the corresponding values for $\bar{D}$ and $\bar{s}$ were extracted from the table. Then the new concentration and the new position of each box boundary were calculated. This process was repeated many times such that the total time spent in sedimentation and diffusion is equal to the duration of the experiment to be simulated. Based on the actual sedimentation time frame, sedimentation velocity profiles at later times were simulated and compared to the corresponding experimental profile.

2.2.4. Equilibrium sedimentation

The high speed, meniscus-depletion procedure [26] was used at 20 °C in a Beckman analytical ultracentrifuge for equilibrium sedimentation. The attainment of equilibrium was tested by the standard procedure [27]. Scans were made at various wavelengths and the baseline correction was made by using absorbance scans at 500 nm. From the absorbance scan, after conversion to appropriate concentration units, the distribution of the protein as a function of radial distance from the center of rotation was calculated and expressed as a plot of C vs. $r^2/2$, where C is the concentration and r is the radial distance. This concentration distribution was fitted to the monomer molecular weight, multimers and equilibrium association constant by employing the NONLIN program [28]. The single isodesmic association model involving association of monomers to yield an equilibrium mixture of linear polymers of indefinite length has also been tested for fitting the data. In this model the free energies of formation of bonds between successive aggregates and monomeric units are equal [23,29–31]. The total concentration (C_T) is $C_1/(1-KC_1)^2$, where K is isodesmic association constant and C_1 is the monomer concentration. Based on this, from the radial distribution of the monomer,

$$C_1(r) = C_{1,0}\exp\left[\sigma\left(r^2/2 - r_0^2/2\right)\right] \tag{13}$$

the radial distribution of the total concentration could be calculated as,

$$C(r) = \frac{C_{1,0}\exp\left[\sigma\left(r^2/2 - r_0^2/2\right)\right]}{1 - KC_{1,0}\exp\left[\sigma\left(r^2/2 - r_0^2/2\right)\right]} + \delta \tag{14}$$

where $C(r)$ is the total concentration at a given radius r, δ is the baseline offset, $C_{1,0}$ is the monomer concentration at the arbitrary reference distance r_0 and σ is the reduced molecular weight

given by,

$$\sigma = \frac{M_1(1-\bar{v}\rho)\omega^2}{RT} \quad (15)$$

where M_1 is the monomer molecular weight, $\bar{v}$ is the partial specific volume, ρ is the solvent density and ω is the angular velocity of the rotor.

2.2.5. Acrylamide quenching

The accessibility of tryptophan residue was monitored as a function of Rev concentration by acrylamide quenching. The quenching of the intrinsic fluorescence due to tryptophan residues of proteins by solute quenchers is a powerful technique to obtain topographical information and to monitor conformational changes of protein molecule. Collisional quenching of fluorescence is described by the Stern–Volmer equation:

$$F_o/F = 1 + k_q\tau_o[Q] = 1 + K_{sv}[Q] \quad (16)$$

where F_o and F are fluorescence intensities in the absence and presence of quencher, respectively, k_q is the bimolecular quenching constant, τ_o is the lifetime of fluorophore in the absence of quencher, $[Q]$ is the concentration of quencher, and $K_{sv} = k_q\tau_o$, is the Stern–Volmer quenching constant. The titration of Rev with acrylamide as a function of Rev concentration was performed at 20 °C using a Perkin-Elmer Luminescence spectrometer LS50. The excitation and emission wavelengths were 295 and 340 nm, respectively. Corresponding titration of 10 mM potassium phosphate buffer containing 1 M sodium chloride at pH 7.4, in which Rev protein of different concentrations has been previously equilibrated by dialysis, was used to correct for the background. Also, titration was performed in 10 mM potassium phosphate buffer at pH 7.4 containing 6 M guanidine hydrochloride and 10 mM DTT, where the tryptophan residues would be completely accessible to the quencher. The cuvette was siliconised to avoid loss of protein by adsorption.

2.2.6. Circular dichroism

Circular dichroic studies in 10 mM potassium phosphate buffer containing 1 M sodium chloride at pH 7.4 were carried out with an Aviv circular dichroism spectrometer model 62S (Lakewood, NJ) under constant nitrogen purging. Ten millimeters pathlength cylindrical quartz cell was used at 1 nm bandwidth setting and the data were collected in the range of 200–300 nm at every 0.5 nm interval. Spectra were recorded as a function of Rev concentration in the range of 3–70 μg/ml (0.2–5 μM). The ellipticity values were expressed as specific ellipticity using corresponding concentrations in g/ml.

2.2.7. ANS-Rev fluorescence

The exposure of hydrophobic surfaces in Rev as a function of protein concentration was monitored by ANS fluorescence. ANS-Rev fluorescence titrations were performed at 20 °C with a Perkin-Elmer Luminescence spectrometer LS50 in 10 mm pathlengths siliconised quartz cells. 0.5–10 μl aliquots of concentrated ANS stock solutions were added to 1 ml of Rev solution in 10 mM potassium phosphate buffer containing 1 M sodium chloride at pH 7.4. The excitation and emission wavelengths were at 350 nm and 480 nm, respectively. The concentration of ANS was determined spectrophotometrically using a value of 6000 M^{-1} cm^{-1} for ε_{351nm}. Corresponding blank titrations were made and the spectra were corrected accordingly. The binding of ANS as a function of increasing ANS concentration at a constant protein concentration was calculated by following the procedure of Horowitz and Criscimagna [32].

$$1/F = 1/n\psi[\text{Rev}]_o + \left(K/n[\text{Rev}]_o\psi\right)\left(1/[\text{ANS}]_0\right) \quad (17)$$

where F is the observed fluorescence intensity; $[\text{ANS}]$ and $[\text{ANS}]_o$ are the free and total concentration of ANS, respectively, and since the ANS concentration was in much excess, $[\text{ANS}] \approx [\text{ANS}]_o$; ψ is the proportionality constant relating the fluorescence intensity to the concentration of the ANS-Rev complex; n is the number of binding sites of ANS; K is the dissociation constant of the complex; and $[\text{Rev}]_o$ is the total concentration of Rev. The plots of $1/F$ vs. $1/[\text{ANS}]$ for different protein concentrations should be linear and should have a common abscissa intercept of $-1/K$.

3. Results

3.1. Protein stability

In order to obtain meaningful and consistent experimental results on the self-association of HIV-1 Rev, it must be first ensured that the system is in a state of rapid reversible equilibrium. Thus, a series of studies was conducted to test the stability of Rev solutions and the proper conditions for storing Rev samples.

Rev solutions at greater than 6 mg/ml, stored in 10 mM potassium phosphate buffer at pH 7.4 containing 1 M NaCl, became cloudy at room temperature (20–23 °C) but cleared once the temperature was reduced to below 4 °C. Dialysis of Rev against relatively low ionic strength buffers, for example, 10 mM potassium phosphate at pH 7.4 containing 0.4 M NaCl, resulted in precipitation of the protein at greater than 3 mg/ml and at room temperature, but not below 4 °C. These phenomena suggest that purified Rev undergoes reversible aggregation that is favored by high temperature and low salt concentration.

Rev solutions stored at 4 °C can undergo protein degradation as indicated by the multiple bands with molecular weights smaller than monomeric Rev. Since no significant change was observed between Rev samples before and after storage for one month at −20 °C, it may be concluded that Rev solutions are stable at −20 °C.

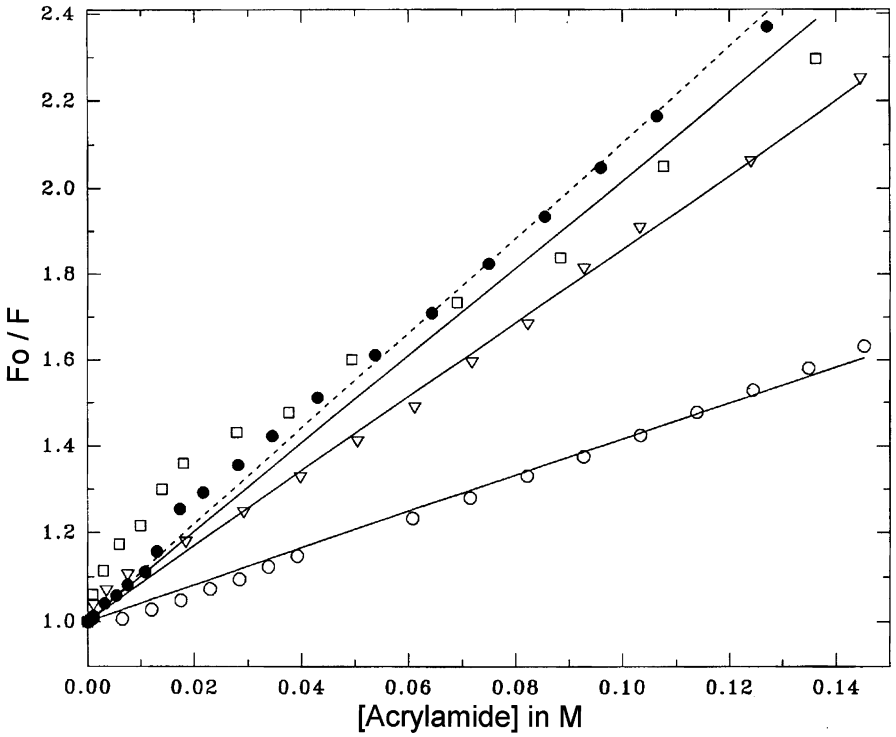

Fig. 1. Fluorescence titration of Rev with acrylamide as a function of Rev concentration at 20 °C. The excitation and emission wavelengths were 295 nm and 340 nm, respectively. Corresponding titration of 10 mM potassium phosphate buffer containing 1 M sodium chloride of pH 7.4, in which Rev protein of different concentrations has been previously equilibrated by dialysis, was used to correct for the background. The symbols (○), (▽) and (□) represent the Rev concentrations 7.5, 0.707 and 0.118 μM, respectively. The lines are the fit of the respective data to Stern–Volmer equation. The symbol (●) represents the data from the experiment done in 10 mM potassium phosphate buffer of pH 7.4 containing 6 M guanidine hydrochloride and 10 mM dithiothreitol. The dashed line is the fit of the data to Stern–Volmer equation.

Based on the information described above, the following studies were performed on freshly dialyzed protein or protein preparation stored at −20 °C and centrifuged at 15 600 *g* for 6 min prior to analysis.

3.2. Free Rev monomer exists in a molten globular form

3.2.1. Acrylamide quenching

As seen in Fig. 1, the slope of the plot of F_o/F vs. [acrylamide] decreases with increasing Rev concentration. A decrease in slope indicates that K_{sv} decreases. A decrease in K_{sv} indicates that the tryptophan residue in Rev is becoming less accessible to acrylamide. The correlation between values of K_{sv} and protein concentration indicates that the accessibility of the fluorophore in Rev is linked to Rev self-association. The K_{sv} value at 0.118 μM Rev is very comparable to that in the presence of 6 M guanidine hydrochloride and 10 mM DTT (Rev concentration 10.7 μM). This result indicates that at very low protein concentration Rev assumes a conformation such that the tryptophan residue is essentially exposed as in an unfolded state. However, this fluorescence study does not provide information on the secondary structures of Rev at this low protein concentration.

3.2.2. Circular dichroism

In order to define the secondary structure of Rev, circular dichroic spectra were taken as a function of Rev concentration. Fig. 2 shows the far ultraviolet circular dichroic spectra at several Rev concentrations. All the spectra have the characteristic minima at 208 and 222 nm. As shown in Fig. 2, specific ellipticity at both 208 and 222 nm increases with increasing Rev concentration and reaching a plateau at approximately 50 μg/ml. The fact that at the lowest Rev concentration studied there is still secondary structure indicates that Rev is not completely unfolded upon dilution.

3.2.3. Rev-ANS fluorescence

Fig. 3 shows the double reciprocal plot of $1/F$ vs. $1/[\text{ANS}]$ at different Rev concentrations. Contrary to the expected common intercept for a non-associating system, the intercepts at the abscissa are dependent on Rev concentration; therefore, the apparent dissociation constants (K) calculated for ANS–Rev complex formed at different Rev concentrations are composites of complex parameters. The apparent value increases with increase in Rev concentration. The inset of Fig. 3 shows that the concentration-normalized fluorescence emission intensity at 480 nm of the ANS–Rev complex

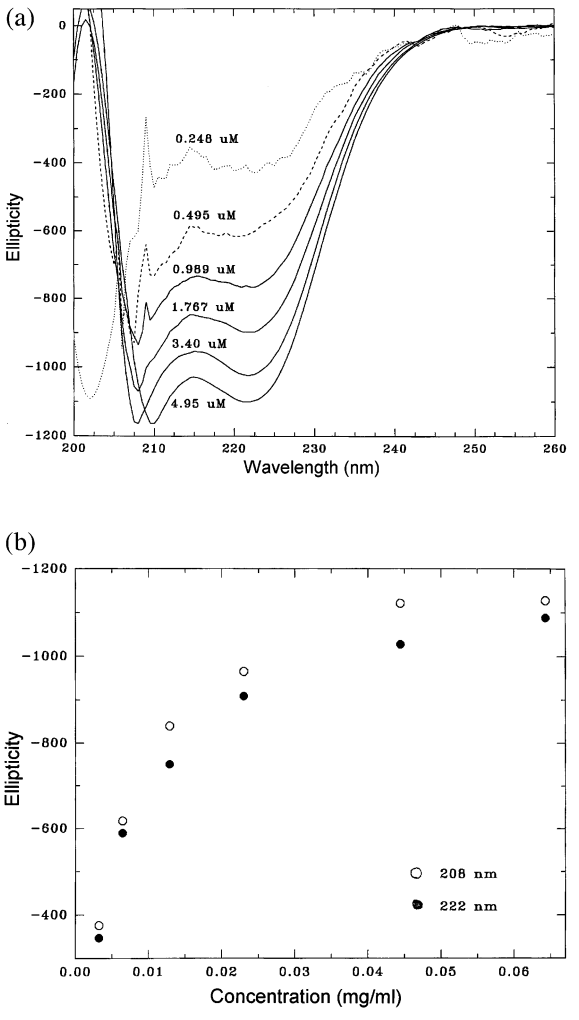

Fig. 2. Far UV circular dichroic spectra of Rev as a function of protein concentration in 10 mM potassium phosphate, 1 M NaCl at pH 7.4 and 20 °C. Protein concentrations are 0.25, 0.5, 0.99, 1.8, 3.4 and 5.0 μM from top to bottom. Relation between ellipticity at 208 and 222 nm as a function of Rev concentration.

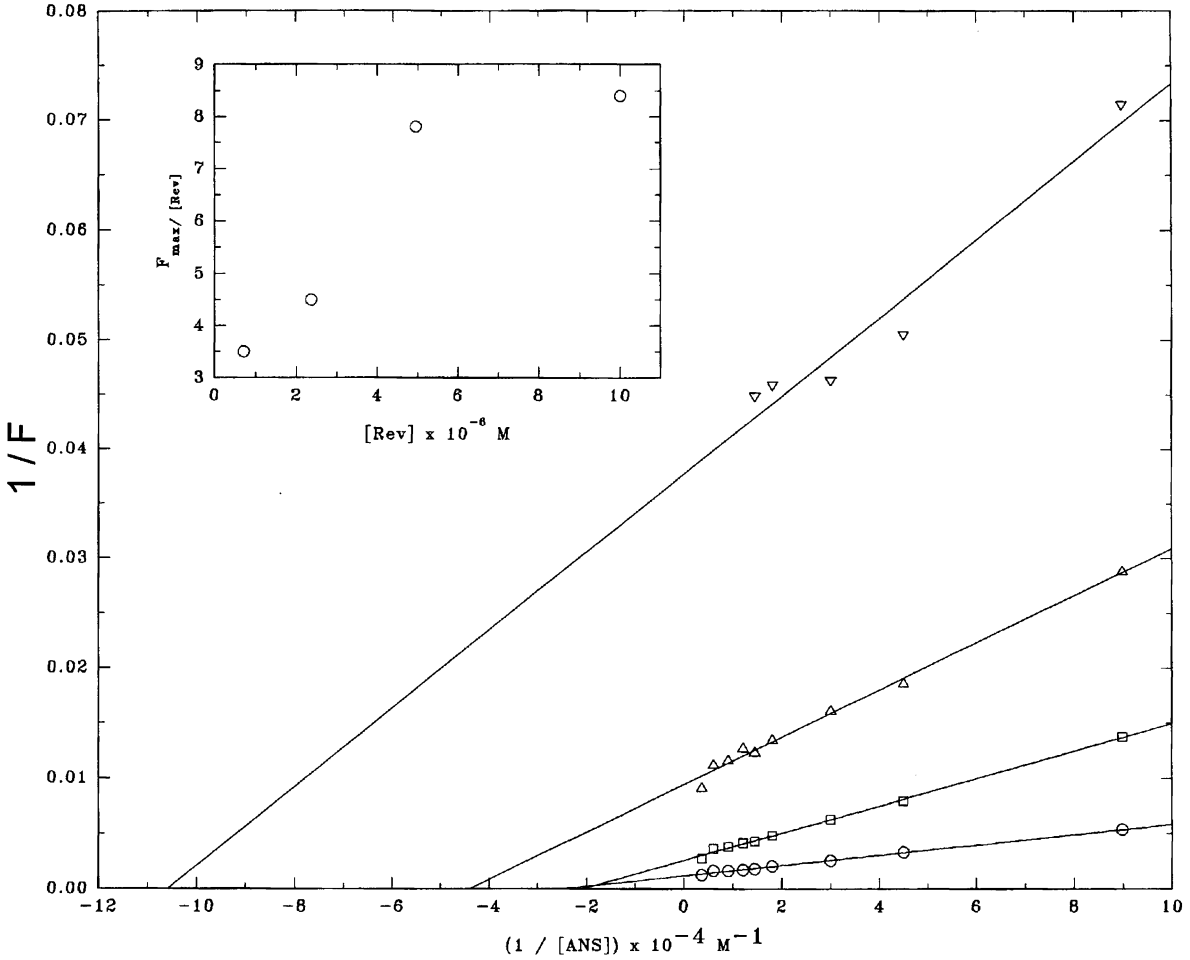

Fig. 3. ANS binding to Rev as a function of Rev concentration in 10 mM potassium phosphate, 1 M NaCl at pH 7.4 and 20 °C. The Rev concentrations are (▽) 0.71 μM, (△) 2.4 μM, (□) 5.0 μM, and (○) 10 μM. The inset shows the relation between Rev concentration and concentration normalized fluorescence emission intensity.

increases with increasing Rev concentration and reaches a plateau at approximately 5 μM.

3.3. Mechanism of self-association

3.3.1. Analytical gel chromatography

As the size of the smallest unit of Rev is one of the key factors that one needs to define to establish the mode of self-association and as the fluorescence detection of the column chromatographic system allows one to perform experiments on samples of lower protein concentration, it is useful to monitor the self-association process of Rev by analytical gel chromatography.

Initial studies were conducted by using small-zone gel chromatography. In each elution profile, the peak was not symmetrical and showed a long trailing edge. This phenomenon has traditionally been interpreted to indicate the presence of self-association although it might also reflect adsorption of gel matrix. Thus, attempts were made to evaluate this self-association reaction by large-zone gel chromatography. A typical gel filtration elution profile of Rev in buffer is shown in Fig.

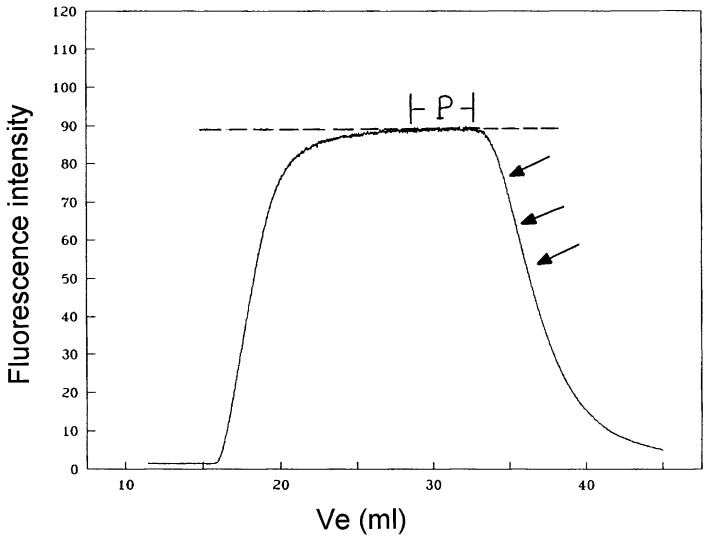

Fig. 4. A typical large zone elution profile of Rev in 10 mM potassium phosphate, 1 M sodium chloride at pH 7.4 and 20 °C. The protein concentration was 3.4 μM. The arrows indicate inflection points and P indicates the plateau.

4, in which it is evident that, the advancing edge was much sharper than its trailing counterpart. It is also interesting to notice that, in the elution profile (Fig. 4), a plateau, indicated by P, was slowly reached after the leading edge. As the chromatography experiments were performed with Rev samples of very low concentration (less than 3.5 μM), one possible reason for this observation is that the percentage of protein adsorbed to the gel matrix, with respect to the total amount of protein loaded, becomes substantial in such low protein concentration range. If this is true, the phenomenon observed in Fig. 4 should be more pronounced with decreasing protein concentration, and the plateau will be expected to be substituted by a broad asymmetric peak below certain protein concentration. This is actually observed in the elution profile of Rev when the protein solution of 0.1 μM was chromatographed under the same conditions. Therefore, it may be concluded that Rev can substantially adsorb to the gel matrix in the experimental protein concentration range. The adsorption of protein to the gel matrix obviates gel chromatography as a tool for studying Rev because adsorption should lead to larger elution volumes.

3.3.2. Velocity sedimentation

In view of the complication encountered in filtration, velocity sedimentation was employed to study the self-association of Rev. Sedimentation experiments were conducted at 20 °C as a function of Rev concentration. In an effort to establish that Rev does indeed undergo rapid re-equilibration, the weight-average sedimentation coefficient, $S_{20,w}$, of Rev, over a range of protein concentrations, was determined at 44 000, 52 000 and 60 000 rev./min. If non-interacting or denatured components of the system were present, the $S_{20,w}$ of Rev sample of fixed concentration would be expected to change as a function of angular velocity [33]. Results showed that the Rev solutions of fixed protein concentrations yield identical values of $S_{20,w}$ at all speeds. It may, therefore, be concluded that within the limits of resolution and under the experimental conditions Rev undergoes rapid self-association.

The concentration dependence of $\bar{S}_{20,w}$ of Rev was determined. The lowest Rev concentration studied was 0.01 mg/ml, below which the resolving capability of the UV scanner does not yield accurate boundary tracings. The value of $S_{20,w}$ was a function of protein concentration, with a smaller

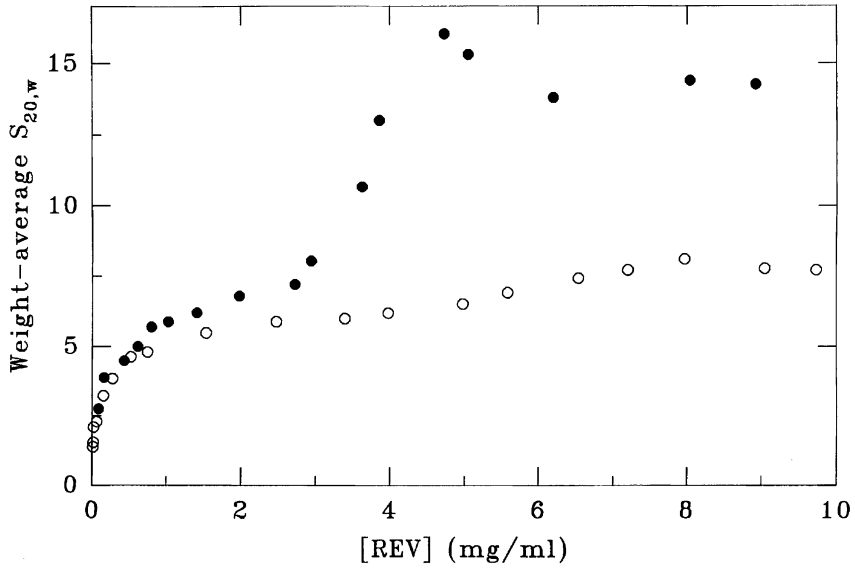

Fig. 5. Concentration dependence of weight-average sedimentation coefficient, $\bar{S}_{20,w}$, of Rev in 10 mM potassium phosphate buffer at pH 7.4 and 20 °C containing (●) 0.42 M NaCl and (○) 1 M NaCl.

value of $\bar{S}_{20,w}$ favored by lower Rev concentration. A $S_{20,w}$ value of 1.37 was obtained at 0.01 mg/ml or 0.77 μM protein concentration. Assuming a spherical shape, this value is close to that predicted for a protein with an apparent molecular weight of 9000, although the monomer molecular weight of Rev is 13 052, based on the protein sequence.

An in depth velocity sedimentation study was carried out in a wide concentration range of 0.01–8 mg/ml of Rev in the presence of two different sodium chloride concentrations (1 and 0.42 M) in 10 mM potassium phosphate buffer at pH 7.4 and 20 °C (Fig. 5). The weight average sedimentation coefficient ($S_{20,w}$) of Rev increases with increasing Rev concentration. The biphasic behavior of $S_{20,w}$ as a function of Rev concentration is notable in both sodium chloride concentrations. This is more pronounced in 0.42 M sodium chloride concentration. This indicates that the mode of Rev self-association is very complex and may include two consecutive reactions. At concentrations above 4.4 mg/ml and 8 mg/ml of Rev in the presence of 0.42 M and 1 M sodium chloride, respectively, the $S_{20,w}$ values decrease significantly, but remained relatively constant, as shown in Fig. 5, implying that at these high Rev concentrations the polymer size is too great and precipitates out of the solution.

The derivative plot of dC/dr vs. radial distance r shows that at low concentrations there is a single slow moving peak (Fig. 6). But as the Rev concentration was increased, the peak became broader and at the same time velocity of this slow peak increased. However, above a certain concentration, the broader peak resolved into a bimodal pattern with the second peak increasing in height/area as the protein concentration was increased further and the area of slow moving peak remained constant. This is characteristic of self-associating system in rapid equilibrium [32]. In an ideal Gilbert system of a rapidly re-equilibrating self association reaction of a protein to form a single high molecular weight polymer with the degree of polymerization, $n \geq 3$, (i) the area under the slow peak in the bimodal profile would remain constant independent of total protein concentration, and (ii) the velocity of the slow peak also would remain constant at a value slightly above that of the velocity of monomer [34–36]. But as seen in Fig. 3, the slow peak is skewed forward at all Rev concentrations with a pronounced increase in the

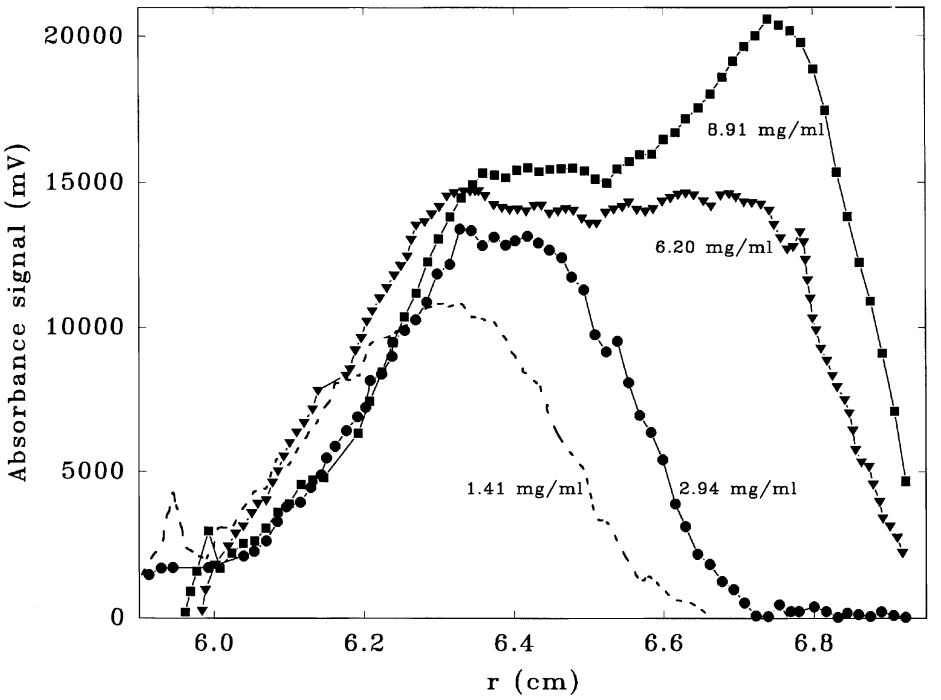

Fig. 6. Sedimentation velocity profiles of Rev expressed as derivative scans in 10 mM potassium phosphate buffer at pH 7.4 and 20 °C containing 0.42 M NaCl. The protein concentrations are 1.4, 2.9, 6.2 and 8.9 mg/ml.

spreading of the peak in the direction of sedimentation. The velocity of this peak increases with increasing Rev concentration. In an ideal monomer↔n-mer equilibrium, where n is ≥ 3, the $S_{20,w}$ vs. protein concentration curve is sigmoidal. However, in the case of Rev, the value of $S_{20,w}$ shows a hyperbolic increase with increase in Rev concentration, e.g. in Fig. 5, up to a concentration of ≈ 3 mg/ml. These are in fact characteristics of a progressive self-associating system. The simplest case of progressive self-association system may be described by a scheme:

$$\begin{aligned} A_1 + A_1 &\leftrightarrow A_2; \quad k_2 = [A_2]/[A_1]^2 \\ A_2 + A_1 &\leftrightarrow A_3; \quad k_3 = [A_3]/\big([A_2][A_1]\big) \\ &\vdots \qquad\qquad \vdots \\ A_{n\text{-}1} + A_1 &\leftrightarrow A_{N_1}; \quad k_n = [A_{N_1}]/\big([A_{n-1}][A_1]\big) \end{aligned} \tag{18}$$

where A_i denotes ith aggregate and k_i is the equilibrium constant. When all k_i's are equal, that is, the free energies of the formation of the successive intermediates are the same $k_2 = k_3 = k_i$, the association is indefinite and is often referred to as an isodesmic self association. In such a case,

$$K_i = i \cdot \big(K_2/2\big)^{i-1} \tag{19}$$

$$K_2 = 2k_2/M_1 = C_2/C_1^2 \tag{20}$$

$$K_1 \equiv 1 \tag{21}$$

where M_1 denotes molecular weight of the monomer and K_i is apparent equilibrium constant transformed to units of ml/mg [31,37–39]. Ideally for a progressive self-association system, the peak should be skewed forward at all protein concentrations. Furthermore, the peak should be broadened, accompanied by increased velocity as the protein concentration is increased. In the case of Rev, as seen in Fig. 6, though the first slow peak can be explained by the above definition as an isodesmic

growth, there is a second fast moving peak appearing in Rev solutions at >3 mg/ml, adding to the complexity of Rev self association. Interestingly the second peak also has the characteristics of the first peak, e.g. the velocity of the second peak increases with peak broadening as the Rev concentration is increased further. This means that there is a second progressive association. This in turn logically forces one to assume an end product for the first isodesmic step (A_{N_1}), which enters the second sequential growing where (A_{N_1}) is the effective monomer species in the model and another stable end product, A_{nN_1}, is formed, analogous to the first polymerization step described by Eq. (18).

$$\begin{aligned} &A_{N_1}+A_{N_1}\leftrightarrow A_{2N_1};\ l_2=[A_{2N_1}]/[A_{N_1}]^2\\ &A_{2N_1}+A_{N_1}\leftrightarrow A_{3N_1};\ l_3=[A_{3N_1}]/\left([A_{2N_1}][A_{N_1}]\right)\\ &\qquad\vdots\qquad\qquad\vdots\\ &A_{(n-1)N_1}+A_{N_1}\leftrightarrow A_{nN_1};\ l_n=[A_{nN_1}]/\left([A_{(n-1)N_1}][A_{N_1}]\right) \end{aligned} \tag{22}$$

where A_{N_1} and A_{nN_1} denote the ith aggregate of the first and second polymerization step, respectively, and l_i is the equilibrium constant of the second polymerization step.

In both progressive association reactions, the formation of end products is favored as $k_n>k_1$ and $l_n>l_i$ [30]. Based on these theories, fitting of the data to various models were done.

3.3.3. Model fitting

To understand the stoichiometry, mechanism and the energetics involved in the Rev self-association, non-linear least squares fitting of weight average sedimentation coefficient data to various models was conducted. Fitting computational algorithms were developed for different possible models not only to fit the data but also to infer the hydrodynamic structure of assembled higher order polymers (Herman, P. unpublished data). Weight average sedimentation coefficient is a function of s_i and C_i, as expressed in Eq. (11).

The total concentration of Rev, C is,

$$C=\sum C_i=\sum K_i C_1^i \tag{23}$$

where C_1 is monomer concentration, which is defined by

$$C_1=\left[\frac{\bar{s}-s_1}{k_i(s_i-\bar{s})}\right]^{1/i-1} \tag{24}$$

for each value of s and the corresponding C is calculated. The non-linear least square method of fitting of Eq. (1) by all the models described here requires good initial estimates of the parameters k_2, l_2, n_2 and n_1. The program then calculates the respective k_i and l_i using the relationship expressed in Eq. (19).

The qualitative analysis of the sedimentation profiles ruled out mechanisms in which the monomeric Rev directly forms higher aggregates and further implied that complex progressive association models are needed to fit the data. The models tested were the simple sequential and a two-step sequential model and multistep model. All these models were tried for all possible stoichiometry to fit the data.

a *Sequential model*: In this model Rev self-association is described by the simplest progressive association, which involves monomer addition, one at a time, to a growing chain of monomers where the free energies of formation of the successive intermediates are the same. This simple single isodesmic association model did not fit simultaneously the experimental data in low and high concentration ranges. However, when the data at the lower concentration range alone were fitted, the fitting was favorable (Fig. 7). This indicated that there is a step function in the association. Thus a two consecutive sequential model was proposed for the self-association reaction.

b *Two-step sequential model*: In this model two distinct isodesmic associations in sequence with an assumption of a stable final end product for the first isodesmic reaction. The second association was modeled as a sequential growing using the stable final end product of first progressive association (A_{N_1}) as the effective monomer species in the model. The model fits

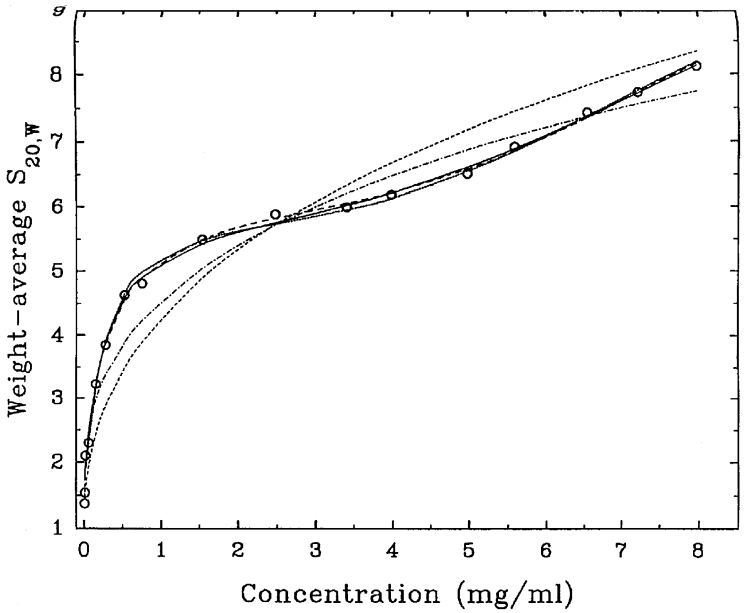

Fig. 7. Fitted curves to the sedimentation velocity in 0.42 M NaCl. The symbols and models are: two-step sequential for spherical or non-spherical intermediates, i.e. s_1 of 1.4 or 0.88, respectively, (solid lines); ring stacking model (long dash line); helical model (dotted line); hybrid model (dot-dash line).

the data obtained in the presence of both 1 M and 0.42 M sodium chloride well. Parameters $k_2=(38\pm8)$ ml/mg, $l_2=(1.8\pm0.5)\times10^{-2}$ ml/mg and the stoichiometry $n_1=11\pm3$, $n_2=5\pm1$ were obtained for 1 M sodium chloride data fitting and parameters $k_2=(56\pm10)$ ml/mg, $l_2=(0.3\pm0.2)$ ml/mg and the stoichiometry $n_1=11\pm3$, and $n_2=16\pm1$ were obtained for 0.42 M sodium chloride data fitting, as summarized in Tables 1 and 2. The step stability function of this model as depicted by the stable end product of the first isodesmic association should be topologically a closed structure formation to prevent further sequential growing. The ring structure formation is the simplest case of that and had already been reported for tubulin [31,40] and tobacco mosaic virus protein [41].

Table 1
Fitting of sedimentation velocity data of Rev in the presence of 1 M sodium chloride

s_1^o	Model	n_1[a]	n_2	k_2 (ml/mg)	l_2 (ml/mg)	SS[b]
1.4 S	Single progressive	12		65		0.0050
1.4 S	Two-step sequential	11	5	38	0.019	0.0048
1.4 S	Ring stacking					0.0082
1.4 S	Helix					0.1387
0.88 S	Two-step sequential	25	4	199	0.139	0.0074
0.88 S	Ring stacking					0.0299
0.88 S	Hybrid					0.0311
0.88 S	Helix					0.0323

[a] n_1 and n_2 are stoichiometry of the end product of the first and second progressive reactions, respectively.
[b] Sum of squares of residuals.

Table 2
Fitting of sedimentation velocity data of Rev in the presence of 0.42 M sodium chloride

s_1^o	Model	n_1[a]	n_2	k_2 (ml/mg)	l_2 (ml/mg)	SS[b]
1.4 S	Two-step sequential	11	16	56	0.324	0.0249
1.4 S	Ring stacking					0.0688
1.4 S	Helix					0.4958

[a] n_1 and n_2 are the stoichiometry of the first and second progressive reactions, respectively.
[b] Sum of squares of residuals.

Different variations of the two-step sequential model were also tried. For example, the ring structure of A_{N1} was modeled as a rigid planer polygon of different geometry and with N1 vertices, where subunits were sequentially placed; a helical rigid spiral structure; and a hybrid of both models. Fitting of all these models to experimental data failed, as indicated by the substantially larger value of SS (Tables 1 and 2). The various fitted parameters for these failed models are not listed in the tables to prevent potential confusion in presentation.

3.3.4. Equilibrium sedimentation

The association mechanism of Rev at low concentration was further studied by sedimentation equilibrium. Rev was subjected to sedimentation equilibrium analysis at 26 000 rev./min. Plots of $\ln C$ vs. r^2 show upward curvature, indicating a concentration dependent association of Rev. Fig. 8 shows simultaneous fitting of equilibrium sedimentation data of various loading concentrations to an isodesmic model. Other discrete simple or complex models could not fit these data. The loading concentrations were in the range of 0.050–0.065

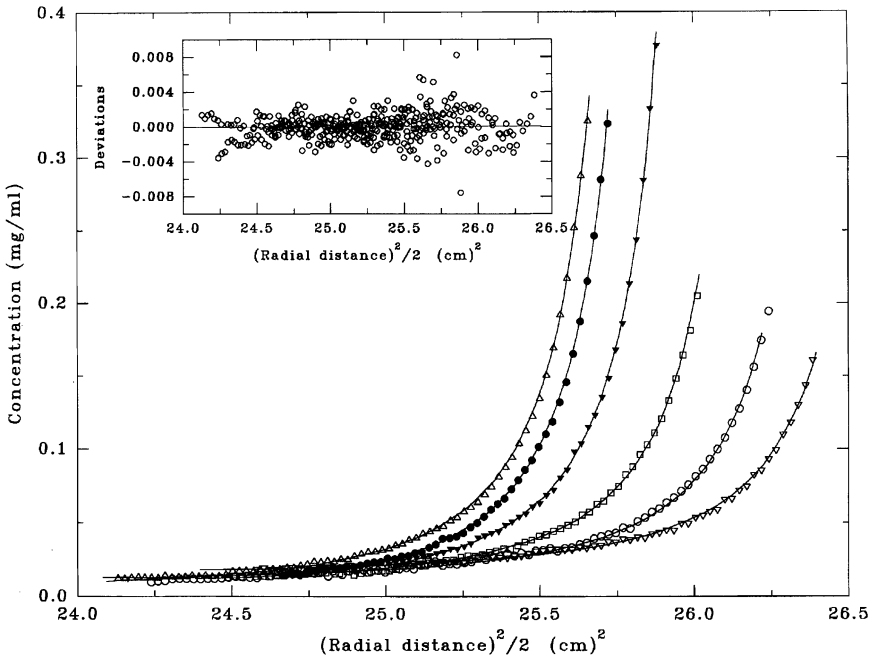

Fig. 8. Concentration distribution of Rev in equilibrium sedimentation in 10 mM potassium phosphate, 1 M NaCl at pH 7.4 and 20 °C. The loading concentrations of Rev range from 50 to 65 μg/ml. The lines are the global fit of data to an isodesmic association model with an association constant of 43±2 ml/mg. The inset shows the distribution of residuals.

mg/ml. A value of 43 ± 2 ml/mg for K_a was obtained by fitting to the isodesmic model. The value of K_a is in good agreement with the value of 38 ml/mg derived from the two-step sequential model using a value of $s_1^o = 1.4$ (Table 1). Thus, the sedimentation equilibrium results substantiate the conclusion derived from the velocity study that the appropriate model is the complex progressive association.

3.3.5. Simulation of velocity sedimentation profile

A derivative plot (dc/dr) of sedimentation boundary is quite informative in identifying the mode of self-association. At any given position in the cell, the sedimentation coefficient depends on the relative concentration of monomer and aggregates present. This in turn is governed by the total concentration and the association parameters. At each point across the boundary, as the total concentration of the solute changes, the concentration of individual species also changes. These changes result in that different parts of the boundary migrate at different rates. As a consequence, the shape of the solute profile is distorted. In the derivative plot, this distortion of solute profile results in distinctive shapes characteristic of different associating modes. Hence, derivative plots representing different modes of association can be simulated. The net result of the simulation iteration procedure is that the derivative plot, which exhibits distinctive shape, can be matched to the experimental plot for immediate qualitative answer. Thus, in order to achieve a more rigorous quantitative analysis of the sedimentation behavior of Rev, the simulated and experimented curves were compared by overlapping one onto the other. This simulation was done for a single isodesmic growth with prolate asymmetry for an initial loading concentration of 0.06 mg/ml, the non-ideality coefficient of 0.0012 ml/mg, the molecular weight of 13 051.5 daltons and the time frame of 6240 s with a rotor speed of 52 000 rev./min. The simulated profiles for the same set of simulation parameters varying only the s_1 value, ranging from 0.88 to 1.4, showed that higher values of s_1 yield sedimentation profiles that deviate more seriously from the experimental pattern at this low protein concentration. This simulation exercise showed that at very low Rev concentration, at which the distribution of free monomeric Rev predominates, a better fitting of the sedimentation velocity profile requires a S_1 value that is less than that of a globular protein.

Table 3
Relationship of hydrodynamics of prolate ellipsoid of rotation for Rev monomer and the ring dimension

s_1^o	f/f_o	a/b	n_1	Ring dimension
1.40 S	1.16	3.72	11	12.1 nm
1.19 S	1.37	6.88	14	15.4 nm
0.96 S	1.70	13.07	21	23.1 nm
0.88 S	1.85	16.48	25	27.6 nm

The hydrodynamic characterization was estimated using the following equation.

$$f/f_o = \frac{M(1-\upsilon\rho)}{s^o_{20,w}\eta\left[162\pi^2 N^2 M(\upsilon+\delta_1\upsilon_1)\right]^{1/3}} \qquad (25)$$

where η is the solvent viscosity, M is the molecular weight of monomer or the sedimenting kinetic unit, N is the Avogadro's number, $\bar{\upsilon}$ is the specific volume of solvent, and δ_1 is the amount of water associated with the protein in $g_{water}/g_{protein}$ [42,43]. The value of δ_1 was calculated based on the method of Kuntz [44] and Hesterberg et al. [45]. For a Rev monomer molecular weight of 13 052 (based on sequence), the frictional ratio (f/f_o) is found to be 1.85. The corresponding axial ratio is 17 for a prolate ellipsoid of revolution and 23 for an oblate ellipsoid of revolution [46]. The values of radius of sphere of equal volume with and without hydration are 1.7 and 1.6 nm, respectively. From a similar calculation for a Rev s_1^o of 1.4 S, the f/f_o is found to be 1.6 and the a/b values are 3.7 and 4.0 for prolate and oblate ellipsoids of revolution, respectively. The values of hydrodynamic characters for other s_1^o are listed in Table 3. Based on the a/b value determined as a function of s_1^o, the rationale for the requirement of more monomers per ring is clear. When the Rev monomers become more and more prolate as the s_1^o is decreased, to cover the same circumference distance of the ring more monomers are required.

4. Discussion

In this study, various spectroscopic and hydrodynamic evidences clearly show that free monomeric Rev in solution undergoes a structural transition upon incorporation into a filamentous polymer.

Rev has only one tryptophan (Trp45). The decrease in accessibility of the tryptophan residue to acrylamide as the Rev concentration increased indicates that the tryptophan is getting buried as new structure(s) is formed. The formation of new structure is directly evidenced by the far ultraviolet spectroscopic study (Fig. 2). With increasing protein concentration the total secondary structural content increases gradually to a limiting value. These observations show that the Rev secondary structure is loosened by partial unfolding or increase in dynamics as its concentration is decreased, confirming the conclusions derived from the results of acrylamide quenching that the Rev reversibly undergoes structural changes as the concentration is increased up to 70 μg/ml (5 μM). The concentration dependent change in Rev secondary structure is further confirmed by the ANS-fluorescence study. The lack of a common abscissa intercept with an increasing Rev concentration clearly shows that as the Rev concentration increases the ANS binding also changes either in the number of ANS bound or in the proportionality factor which is a reflection of the environment of the ANS binding site. However, above 5 μM of Rev, as seen in Fig. 3, the lines converge on to a common abscissa intercept. Similarly the concentration-normalized fluorescence intensity above 5 μM Rev seems to be unchanged. It has been reported that ANS binds more strongly to molten globule state than to native and completely unfolded states [47]. The observation of a decrease in K value on decreasing Rev concentration is supportive evidence for such an interpretation that Rev most likely assumes a molten globule state at low Rev concentration. On the other end, the increase in K value on increasing the Rev concentration is most likely due to secondary structural changes tending more towards a native state. This conclusion is further strengthened by the results of the far ultraviolet circular dichroic studies that show Rev forming more α-helical structure as evidenced by increase in ellipticity at 208 and 222 nm. ANS does not bind significantly to α-helical structure as inferred from model compound studies [47]. A protein concentration-dependent structural change indicates the presence of a linked reaction.

This concentration dependent structural transition is directly related to self-association of Rev. Within this concentration range, data from both the sedimentation equilibrium and velocity study consistently indicate that Rev undergoes a progressive assembly process, an observation that is in agreement with the report by Cole et al. [48].

Simulation of velocity sedimentation patterns of proposed models of self-association is used to confirm the model by comparing the theoretical sedimentation patterns with the velocity sedimentation profiles [23,24,49,50]. The associating system is considered to be in chemical equilibrium everywhere in the cell throughout the run and it is essentially equivalent to the sedimentation of a single concentration dependent solute [50]. The method assumes no effects like time dependent changes of the properties of protein or pressure dependence of equilibrium constants. Interestingly, the results from the study employing sedimentation equilibrium are consistent with the sedimentation velocity data at low Rev concentration range for a simple progressive model, confirming the conclusion by velocity sedimentation studies that Rev self-associates by progressive association at low concentration range. The maximum concentration of the equilibrium sedimentation concentration gradient is within the Rev concentration range that fits well by the first progressive reaction of the two-step sequential model. Indeed, the equilibrium constant (42 ml/mg) obtained by equilibrium sedimentation is close to the value of 38 ml/mg obtained for fitting experimental $S_{20,w}$ values in the Rev concentration range of 0–8 mg/ml. It is also close to the value of 65 ml/mg for single progressive model fitting in the concentration range of 0–3.6 mg/ml, taking 1.4 S as the s_1^o. The difference in the values could stem from the fact that in the fitting of experimental $S_{20,w}$ by either the single or two-step progressive model one or two closed-structure end products were involved

while in the fitting of the equilibrium sedimentation data the single progressive growth of Rev polymer was open ended. Irrespective of this quantitative difference, these sedimentation data clearly confirm that progressive association is the mechanism of self-association and in the low Rev concentration range a model of single progressive growth can fit the data well.

The better fit of the value of s_1^o for free Rev monomer is 0.88 S, which is much lower than 1.4 S. The fitting parameters obtained based on 1.4 S seem to be consistent with the equilibrium sedimentation study and the literature electron microscopic studies. The electron microscopic studies [5,6] show that Rev forms filamentous structure of 14 nm wide. This dimension can be taken as the diameter of the ring structure. Based on the stoichiometry of monomers per ring and the hydrodynamic calculation, the ring dimension can be calculated for each fitting (Table 3). In the presence of either 0.42 or 1 M sodium chloride, for the single progressive model and fitting in the concentration range of 0–3.6 mg/ml with an end product, the diameter of the end product was calculated to be 16.5 nm. For the two-step progressive model and fitting of the entire concentration range a value of 12.1 nm was obtained. These values are very close to the literature value of 14 nm. This result indicates that the ring dimension is independent of sodium chloride concentration. Also, in all cases the s_1^o is 1.4 S. In comparison, in the case of fitting stoichiometry based on the s_1^o value of 0.88 S, the diameter of the ring was calculated to be 27.5 nm, which is far off from the value obtained by electron microscopic studies, although simulation studies imply that a smaller value of s_1 fit the sedimentation profile at low protein concentration better. What could be the reason for this inconsistency? This can be explained by analyzing the spectroscopic results. This concentration dependent transition from unfolded to folded state is directly related to the self-association of Rev. As the association is confirmed to be progressive, it is clear from above that structural changes occur for each addition of monomer. The weight percent of ring formed at the concentration of 60 μg/ml is negligible as compared to the monomer and lower intermediates present. Thus, the s_1^o value of 0.88 S, obtained by simulation study at a concentration where the presence of free monomeric Rev dominates, does not yield results that agree with those acquired from the equilibrium sedimentation and electron microscope studies. On the other hand, using $s_1^o = 1.4$ S yields results that support these latter studies well and the value of 1.4 S is arrived at by an assumption that Rev monomer is globular. The fact that the simulation study does not support this value indicates that free Rev monomer is not a tightly packed globular particle, a conclusion in complete agreement with the spectroscopic data. Results of these spectroscopic and hydrodynamic studies indicate that Rev probably undergoes transition from a molten globule to a more compact state as it is assembled onto the polymeric form, although according to the definition of Ptitsyn [51] molten globule state changes occur at tertiary structure level and there is no significant unfolding–folding for the molten globule to native state transition.

The specific structures, rings, filaments and bundle of filaments predicted by the present study are present in vivo as reported by the electron microscope studies [5–7]. Rev filaments have been thought to package viral mRNA and thus physically protect it from splicing. This packaging has also been reported. These Rev filaments, which are involved in transporting the packaged RNA to polysomes, may utilize an active transport system similar to ribonucleoprotein particles [52,53]. Reports that the biological activity requires a threshold level of Rev in vivo directly support the concentration dependence of self-association of Rev [54]. Though self-association is required for its biological function of RNA packaging and transport, the self-association is independent of RNA. Similar situations are seen in the cases of viral capsid protein [55], TMV coat protein [56] and *E. coli* Rec A [57].

In summary, the present in vitro study on the self association of Rev provides data that are consistent with the literature that Rev undergoes a complex mode of self association leading to filamentous structures that resemble those observed by electron microscopy.

Acknowledgments

Supported by NIH grant GM-45579, Robert A. Welch Foundation grants H-1238 and H-0013 and a grant from the John Sealy Memorial Endowment Fund for Biomedical Research.

References

[1] T.J. Daly, K.S. Cook, G.S. Gray, T.E. Malione, J.R. Rusche, Specific binding of HIV-1 recombinant rev protein to the RRE in vitro, Nature 342 (1989) 816–819.

[2] M.H. Malim, J. Hauber, R. Fenrick, S. Bohnlein, B.R. Cullen, Nuclear export of unspliced HIV-1 mRNAs is regulated by the viral rev trans-activator, Human Retroviruses, Alan R. Liss, Inc, 1990, pp. 97–108.

[3] G.N. Pavlakis, B.K. Felber, M. Hadzopoulou Cladaras, C. Cladaras, A. Athanassopoulos, C.M. Drysdale, A novel mechanism of gene regulation: the rev protein of HIV-1 increases the transport and half-life of the viral mRNAs containing a predicted highly structured rev-responsive element (RRE), Human Retroviruses, Alan R. Liss, Inc, 1990, pp. 141–152.

[4] M.H. Malim, S. Bohnlein, J. Hauber, B.R. Cullen, Functional dissection of the HIV-1 rev trans-activator-derivation of a trans-dominant repressor of rev function, Cell 58 (1989) 205–214.

[5] S. Heaphy, J.T. Finch, M.J. Gait, J. Karn, M. Singh, Human immunodeficiency virus type 1 regulator of virion expression, rev, forms nucleoprotein filaments after binding to a purine-rich 'bubble' located within the rev-responsive region of viral mRNAs, Proc. Natl. Acad. Sci. USA 88 (1991) 7366–7370.

[6] J. Karn, C. Dingwell, J.T. Finch, S. Heaphy, M.J. Gair, RNA binding by the tat and rev proteins of HIV-1, Biochimie 73 (1991) 9–16.

[7] P.T. Wingfield, S.J. Stahl, M.A. Payton, S. Venkatesan, M. Misra, A.C. Steven, HIV-1 Rev expressed in recombinant Escherichia coli: purification, polymerization, and conformational properties, Biochemistry 30 (1991) 7527–7534.

[8] Surendran, R., Cheng, Z., Herman, P., Lee, J.C., Formation of HIV-1 Rev polymers. Presented in the 7th Gibbs conference on Biological Thermodynamics, Carbondale, IL, USA (1993) p. 38.

[9] M.H. Malim, B.R. Cullen, HIV-1 structural gene expression requires the binding of multiple rev monomers to the viral RRE: Implications for HIV-1 latency, Cell 65 (1991) 241–248.

[10] H.S. Olsen, A.W. Cochrane, P.J. Dillon, C.M. Nalin, C.A. Rosen, Interaction of the human immunodeficiency virus type 1 Rev protein with a structured region in env mRNA is dependent on multimer formation mediated through a basic stretch of amino acids, Genes Dev. 4 (1990) 1357–1364.

[11] M.L. Zapp, T.J. Hope, T.G. Parslow, M.R. Green, Oligomerization and RNA binding domains of the type 1 human immunodeficiency virus rev protein: a dual function for an arginine-rich binding motif, Proc. Natl. Acad. Sci. USA 88 (1991) 7734–7738.

[12] M.H. Malim, B.R. Cullen, Rev and the fate of pre-mRNA in the nucleus: implications for the regulation of RNA processing in eukaryotes, Mol. Cell. Biol. 13 (1993) 6180–6189.

[13] J. Kjems, P.A. Sharp, The basic domain of rev from human immunodeficiency virus type 1 specifically blocks the entry of U4/U6·U5 small nuclear ribonucleoprotein in spilceosome assembly, J. Virol. 67 (1993) 4769–4776.

[14] J. Kjems, A.D. Frankel, P. Sharp, Specific regulation of mRNA splicing in vitro by a peptide from HIV-1 rev, Cell 67 (1991) 169–178.

[15] U. Fischer, S. Meyer, M. Teufel, C. Heckel, R. Luhrmann, G. Rautmann, Evidence that HIV-1 rev directly promotes the nuclear export of unspliced RNA, EMBO J. 13 (1994) 4105–4112.

[16] N. Richard, S. Iacampo, A. Cochrane, HIV-1 rev is capable of shuttling between the nucleus and cytoplasm, Virol. 204 (1994) 123–131.

[17] D.M. D'Agostino, B.K. Felber, S.E. Harrison, G.N. Pavlakis, The rev protein of human immunodeficiency virus type 1 promotes polysomal association and translation of gag/pol and vpu/env mRNAs, Mol. Cell. Biol. 12 (1992) 1375–1386.

[18] Y. Luo, H. Yu, B.M. Peterlin, Cellular protein modulates effects of human immunodeficiency virus type 1 rev, J. Virol. 68 (1994) 3850–3856.

[19] M. Ruhl, M. Himmelspach, G.M. Bahtr, F. Hammerschmid, H. Jaksche, B. Wolff, et al., Eukaryotic initiation factor 5A is a cellular target of the human immunodeficiency virus type 1 rev activation domain mediating trans-activation, J. Cell Biol. 123 (1994) 1309–1320.

[20] S.S. York, R.C. Lawson, D.M. Worah, Binding of recrystallized and chromatographically purified 8-anilino-1-naphthalenesulfonate to *Escherichia coli* lac repressor, Biochemistry 17 (1978) 4480–4486.

[21] R.N. Fergusson, H. Edelhoch, H.A. Saroff, J. Robbins, H.J. Cahnmann, Negative cooperativity in the binding of thyroxine to human serum prealbumin, Biochemistry 14 (1975) 282–289.

[22] T.J. Daly, R.C. Doten, P. Rennert, M. Auer, H. Jaksche, A. Donner, et al., Biochemical characterization of binding of multiple HIV-1 Rev monomeric proteins to the Rev responsive element, Biochemistry 32 (1993) 10 497–10 505.

[23] R.R. Holloway, D.J. Cox, Computer simulation of sedimentation in the ultracentrifuge. VII. Solutes undergoing indefinite self-association, Arch. Biochem. Biophys. 160 (1974) 595–602.

[24] D.J. Cox, R.S. Dale, Simulation of transport experiments for interacting systems, in: C. Frieden, L.W. Nicol

(Eds.), Protein-Protein Interactions, John Wiley and Sons, New York, 1981, pp. 173–211.
[25] R.F. Steiner, Reversible association processes of globular proteins.7.The reversible dimerization of chymotrypsin, Arch. Biochem. Biophys. 49 (1954) 400–416.
[26] D.A. Yphantis, Equilibrium ultracentrifugation of dilute solutions, Biochemistry 3 (1964) 297–317.
[27] H.K. Schachman, S.J. Edelstein, Ultracentrifuge studies with absorption optics. IV. Molecular weight determinations at the microgram level, Biochemistry 5 (1966) 2681–2705.
[28] M.L. Johnson, J.J. Correia, D.A. Yphantis, H.R. Halvorson, Analysis of data from the analytical ultracentrifuge by non-linear least- squares techniques, Biophys. J. 36 (1981) 575–588.
[29] E.T. Adams Jr, M.S. Lewis, Sedimentation equilibrium in reacting systems. VI. Applications to indefinite self-associations. Studies with.beta.-lactoglobulin A, Biochemistry 7 (1968) 1044–1053.
[30] K.E. Van Holde, G.P. Rossetti, A sedimentation equilibrium study of the association of purine in aqueous solutions, Biochemistry 6 (1967) 2189–2194.
[31] R.P. Frigon, S.N. Timasheff, Magnesium-induced self-association of calf brain tubulin. I. Stoichiometry, Biochemistry 14 (1975) 4559–4566.
[32] P.M. Horowitz, N.L. Criscimagna, Differential binding of the fluorescent probe 8-anilinonaphthalene-2-sulfonic acid to rhodanese catalytic intermediates, Biochemistry 24 (1985) 2587–2593.
[33] W.F. Stafford, Analysis of reversibly interacting macromolecular systems by time derivative sedimentation velocity, Method Enzymol. 323 (2000) 302–325.
[34] G.A. Gilbert, Discuss. Faraday Soc. 20 (1955) 68–71.
[35] G.A. Gilbert, Sedimentation and electrophoresis of interacting substances I, Proc. R. Soc. Lond. A 250 (1959) 377–388.
[36] R. Townend, R.J. Winterbottom, S.N. Timasheff, Molecular interactions in β lactoglobulin. II. Ultracentrifugal and electrophoretic studies of the association of β lactoglobulin below its isoelectric point, J. Am. Chem. Soc. 82 (1960) 3161–3168.
[37] P.W. Chun, S.J. Kim, C.A. Stanley, G.K. Ackers, Determination of the equilibrium constants of associating protein systems. III. Evaluation of the weight fraction of monomer from the weight-average partition coefficient (application to bovine liver glutamate dehydrogenase), Biochemistry 8 (1969) 1625–1632.
[38] P.W. Chun, S.J. Kim, Determination of the equilibrium constants of associating protein systems. IV. Application of the weight-average partition coefficient to analysis of BM1 non-ideality term (as applied to bovine liver L-glutamate dehydrogenase), Biochemistry 8 (1969) 1633–1643.
[39] E. Reisler, J. Pouyet, H. Eisenberg, Molecular weights, association, and frictional resistance of bovine liver glutamate delydrogenase at low concentrations, Biochemistry 9 (1970) 3095–3102.
[40] S.N. Timasheff, The self-assembly by long rodlike structures, in: C. Frieden, L.W. Nicol (Eds.), Protein-Protein Interactions, John Wiley and Sons, New York, 1981, pp. 315–316.
[41] G. Stubbs, in: F.A. Jurnak, A. McPherson (Eds.), Biological Macromolecules and Assemblies, 1, John Wiley and Sons, New York, 1984, pp. 149–202.
[42] H. Fujita, Mathematical Theory of Sedimentation Analysis, Academic Press, New York, 1962.
[43] J.T. Edsall, in: H. Neurath, K. Bailey (Eds.), The Protein, 1B, Academic Press, New York, 1953, pp. 549–726.
[44] I.D. Kuntz, Hydration of macromolecules. III. Hydration of polypeptides, J. Am. Chem. Soc. 93 (1971) 514–516.
[45] L.K. Hesterberg, J.C. Lee, H.P. Erickson, Structural properties of an active form of rabbit muscle phosphofructokinase, J. Biol. Chem. 256 (1981) 9724–9730.
[46] T. Svedberg, K.O. Pederson, The Ultracentrifuge, Claredon Press, Oxford, England, 1940.
[47] G.V. Semisotnov, N.A. Rodionova, O.I. Razgulyaev, V.N. Uversky, A.F. Gripas, R.I. Gilmanshin, Study of the molten globule intermediate state in protein folding by a hydrophobic fluorescent probe, Biopolymers 31 (1991) 119–128.
[48] J.L. Cole, J.D. Gelman, J.A. Shafer, L.C. Kuo, Solution oligomerization of the rev protein of HIV-1: implications for function, Biochemistry 32 (1993) 11 769–11 775.
[49] L.M. Gilbert, A.G. Gilbert, Sedimentation velocity measurement of protein association, Method Enzymol. 27 (1973) 273–296.
[50] D.J. Cox, Calculation of simulated sedimentation velocity profiles for self-association solutes, Method Enzymol 48 (1978) 212–242.
[51] O.B. Ptitsyn, The molten globule state, in: T.E. Creighton (Ed.), Protein Folding, W.H. Freeman and Company, New York, 1992, pp. 243–300, Chapter 6.
[52] P. Silver, H. Goodson, Nuclear protein transport, CRC Crit. Rev. Biochem. Mol. Biol. 24 (1989) 419–435.
[53] C.M. Starr, J.M. Hanover, Structure and function of the nuclear pore complex: new perspectives, BioEssays 12 (1990) 323–330.
[54] R.J. Pomerantz, D. Trono, M.B. Feinberg, D. Baltimore, Cells non-productivity infected with HIV-1 exhibit an aberrant pattern of viral RNA expression, Cell 61 (1990) 1271–1276.
[55] S.C. Harrison, in: B.N. Fields, D.M. Knipe (Eds.), Virology, Raven Press Ltd, New York, 1990, pp. 37–61.
[56] J. Butler, The current picture of the structure and assembly of tobacco mosaic virus, J. Gen. Virol. 65 (1984) 253–279.
[57] S.L. Brenner, A. Zlotnick, J.D. Griffith, RecA Protein self-assembly, J. Mol. Biol. 204 (1988) 959–972.